Journal of Solid State Chemistry **156,** 220–224 (2001)
doi:10.1006/jssc.2000.8991, available online at http://www.idealibrary.com on IDEAL®

Preparation, Characterization, and Low-Temperature Heat Capacities of Nanocrystalline TiO_2 Ultrafine Powder

Xin-Ming Wu,*,† Lan Wang,† Zhi-Cheng Tan,† Guang-Hai Li,‡ and Song-Sheng Qu*,[1]

*College of Chemistry and Environmental Science, Wuhan University, Wuhan 430072; † Thermochemistry Laboratory, Dalian Institute of Chemical Physics, Chinese Academy of Sciences, Dalian 116023; and ‡ Institute of Solid State Physics, Chinese Academy of Sciences, Hefei, Anhui 230031, People's Republic of China

Received March 23, 2000; in revised form August 2, 2000; accepted October 6, 2000; published online December 21, 2000

Nanocrystalline TiO_2 ultrafine powders with different grain sizes have been prepared by the sol–gel method. The grain sizes and the crystalline phases have been determined. Heat capacities in the temperature range of 78–370 K have also been measured, and the polynomial equations expressing the change of heat capacity with temperature were fitted. The obtained values of the heat capacity have been compared with those of the bulk crystal from the literature. The relations between heat capacity and the grain size of nanocrystalline TiO_2 have been discussed in terms of energy. © 2001 Academic Press

Key Words: **nanocrystalline TiO_2; grain size; crystalline phase; low-temperature heat capacity.**

1. INTRODUCTION

In recent years, with the development of fine chemical industries and precision electronic ceramic materials, the requirements and demand for ultrafine powder materials has become higher and higher. Due to the properties of ultrafine powder of high specific surface and high reaction activity, it has been widely used in the fields of semiconductive ceramics and photocatalysts, for instance in ferroelectric and piezoelectric ceramics and in pressure-sensitive, gas-sensitive, and temperature-sensitive elements (1, 2). With the development of modern science and technology, the applied and theoretical research of nanocrystalline TiO_2 has been further carried out (3).

The heat capacity of bulk TiO_2, as its important thermodynamic property, has been previously reported. However, the heat capacity of nanocrystalline TiO_2 and the relations between it and thermodynamic properties, especially at low temperature, have not been reported in the literature up to now. This paper aims to present the preparation, the characterization, and the low-temperature heat capacity of nanocrystalline TiO_2 ultrafine powder, prepared by sol–gel processing. The relations among the energy, the heat capacities, the grain sizes, and the different crystalline phases of ultrafine powder have been analyzed.

[1] To whom correspondence should be addressed. Fax: (86) 027-87647617. E-mail: ipc@whu.edu.cn.

2. EXPERIMENT

2.1. Sample Preparation

Two samples were prepared by the sol–gel method, in which butyl titanate was used as raw material, absolute alcohol as solvent, glacial acetic acid as chelating agent, and hydrochloric acid as catalyst (2, 4). At room temperature, 10 vol of $Ti(OBu)_2$, 1 vol of glacial HAc, and 20 vol of absolute C_2H_5OH were mixed as original solution. Then, 10 vol of absolute C_2H_5OH and a certain amount of water, whose molar number doubled that of the titanate, were mixed, and the pH was adjusted to about 4 with HCl as the titration solution. The titration experiment was done gently with stirring and maintenance of the pH of the solution at $4 \sim 5$ with HCl. It ended when the colloid had no fluidity.

The colloid was slowly dried under 100°C for about 6 h so as to obtain yellow dried gel powder. The obtained dry gel powder was further ground and divided into two parts. The heat treatment of the first part was at 500°C for 2 h and that of the second was at 900°C for 4 h (2).

The third sample was prepared by weighing 20 g of ilmenite and adding 8 ml of 18.4 mol L^{-1} dense H_2SO_4 to it and letting it dissolve for 2 h under 80°C. Then we added 100 ml of water to it and allowed it hydrolyze completely. The white deposition of H_2TiO_3 was obtained. Nonionic water was used to wash the deposition of H_2TiO_3 until no SO_4^{2-} was detected. The deposition was dried under 80°C, and finally it received heat treatment at 550°C for 2 h (5).

All reagents used were A.R.

To prevent the samples from deliquescing, the prepared samples were put into three bottles, respectively. Then these bottles were filled with He gas after being vacuumed.

0022-4596/01 $35.00
Copyright © 2001 by Academic Press
All rights of reproduction in any form reserved.

2.2. Measurement of the Grain Size, the Crystalline Phase, and the Purity of the Samples

The grain sizes and crystalline phases were determined and characterized by an RU-200 X-ray diffractometer manufactured by Rigaku, Japan. The experimental conditions were as follows: Cu$K\alpha$ radiation; tube voltage/current, 20 kv/30 mA; scanning range (2θ), 5 ~ 80°; scanning speed, 5°/min. The impurity contents of the samples were determined with an ICP plasma spectrometer.

2.3. Measurement of the Heat Capacity of the Samples

The heat capacities of the samples were measured with a precision automatic adiabatic calorimeter established in our lab. The sample cell was made of a gold-plated copper cylinder with a volume of ca. 6 ml. A gold-plated Y-shaped vane was fixed in the sample cell in order to shorten the heat equilibrium time. The Karma wire used for heating the sample was wound on the outer surface of the sample cell. The temperature of the sample cell was determined with a precision platinum resistance thermometer. The inner and outer shields were covered with brilliant aluminum foil to prevent heat radiation. High vacuum (ca. 1.33×10^{-2} Pa) within the shields was used to prevent heat conduction. Furthermore, an automatic heat trace with synchronized thermocouple signal was applied to prevent the conduction and radiation of the heat. The structure of the adiabatic calorimeter was described previously (6). When the sample was put into the sample cell, the lid was sealed with cycleweld for solidification for 24 h. The sample cell was vacuumed and filled with He gas until atmospheric pressure was reached, to maintain good thermal conduction (7). Finally, the sample cell was fixed into a container. The determination of the temperature was from the temperature region of liquid nitrogen to 370 K. The process of the determination of heat capacities and the calculation of experimental results were completed automatically by a computer. The time of the experiment was about 38 h per sample.

3. RESULTS AND DISCUSSION

3.1. The Grain Size and the Crystalline Phase of TiO_2 Powder

The X-ray diffraction patterns of the three crystal powder samples are shown in Fig. 1.

The 2θ values and peak widths of the highest peaks at the half-height of the three samples were measured by X-ray broadening analysis (8). The average grain size was calculated from the Scherrer formula: $D = K\lambda/B \cos\theta$, where D is the average grain size (nm), K is Scherrer's constant, also called the shape factor, $K = 0.89$ (9), λ is the wavelength of the X-ray (nm), B is peak width at half-height (rad), and θ is the Bragg angle (°). The calculated results show that the

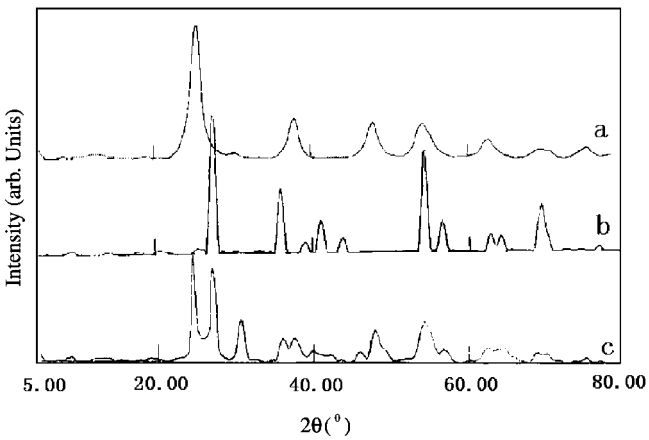

FIG. 1. The XRD patterns of TiO_2 at various nanometer sizes: (a) 15, (b) 75, and (c) 14 nm.

average grain sizes of the first two samples were 15 and 75 nm, respectively, and the third was 14 nm.

It was concluded that 15-nm TiO_2 powder was a nanocrystal in the anatase phase, 75-nm TiO_2 powder was a nanocrystal in the rutile phase, and 14-nm TiO_2 powder was a mixture of the anatase and rutile phases, when the X-ray diffraction diagrams of the three powder samples were compared with the standard cards of TiO_2 powder diffraction. By the calculation of the matrix-flushing method (10), the relative content of the rutile-phase TiO_2 powder is 47.5% and that of the anatase-phase TiO_2 powder is 52.5% in the third sample.

3.2. Purity of Nanocrystalline TiO_2 Powder

The impurity content of TiO_2 ultrafine powder was determined with an ICP plasma spectrometer. The results are listed in Tables 1 and 2.

The results in the tables demonstrate that the purity of all samples was higher than 99.9%. This means that the purity of nanocrystalline powder can meet the demands of practical application.

3.3. Lattice Constants and Axial Ratios of Nanocrystalline TiO_2

The TiO_2 crystalline phase belongs to the tetragonal system. The lattice constants and the axial ratios of the first

TABLE 1
Purity Analysis of TiO_2 Ultrafine Powder in the Anatase Phase at 15 nm and in the Rutile Phase at 75 nm (w/10^{-6})

Element:	Cl	Na_2O	Fe_2O_3	Li_2O	Mg	Al_2O_3
Content	100	41	28	37	—	—

TABLE 2
Purity Analysis of TiO_2 Ultrafine Powder at 14 nm (w/10^{-6})

Element:	Cl	Na_2O	Fe_2O_3	Li_2O	Mg	Al_2O_3
Content	100	76	40	42	—	—

two samples were calculated with the following formula:

$$\frac{1}{d^2(hkl)} = \frac{h^2}{a_0^2} + \frac{k^2}{b_0} + \frac{l^2}{c_0}.$$

Results show that the unit cell parameters of the anatase are $a = 0.4977$, $c = 0.4998$, $c/a = 1.0042$, and that of rutile are $a = 0.4982$, $c = 0.4981$, $c/a = 0.9999$. That is to say, the distortion of the 15-nm anatase TiO_2 lattice is bigger than that of the 75-nm rutile TiO_2.

3.4. Heat Capacity and C_p–T Polynomial Equation of Nanocrystalline TiO_2 Powder

In the heat capacity measurement, 250 experimental points were obtained in the temperature range 78–370 K. The heat capacity values of bulk crystal TiO_2 were cited from the literature (11), which gave data on the heat capacities vs temperatures and the corresponding C_p–T curves of the anatase and the rutile phases, respectively.

The homemade precision automatic adiabatic calorimeter was calibrated with the calorimetric standard substance α-Al_2O_3. The inaccuracy is within $\pm 0.1\%$ (12). During the equilibrium period of the sample cell, the temperature drift rate usually can be stabilized to 10^{-4} K/min. The temperature increment was controlled at 2–5 K. The data obtained in the experiment are listed in Tables 3, 4, and 5, respectively.

The plot of the measured heat capacities vs temperature is shown in Fig. 2. Only the anatase-phase TiO_2 is shown in Fig. 2 because of the near superposition of two bulk crystal C_p–T curves in the literature.

The polynomial equations of the change of heat capacity with temperature were obtained by the least-square method.

For 14-nm ultrafine powder of TiO_2,

$$C_p = 57.314 + 32.904X - 4.5667X^2 + 5.9816X^3 - 0.37166X^4 \quad (\mathrm{J\,K^{-1}\,mol^{-1}}), \qquad [1]$$

where $X = (T - 223.46)/144.45$.

For 15-nm ultrafine powder in the anatase phase,

$$C_p = 57.412 + 29.603X - 3.2015X^2 + 6.4598X^3 - 1.6607X^4 \quad (\mathrm{J\,K^{-1}\,mol^{-1}}), \qquad [2]$$

where $X = (T - 225.41)/145.23$.

TABLE 3
The Measured Heat Capacity Values of 15-nm Anatase TiO_2 Ultrafine Powder, C_p ($\mathrm{JK^{-1}\,mol^{-1}}$) ($M = 79.8988$)

T (K)	C_p ($\mathrm{JK^{-1}\,mol^{-1}}$)	T (K)	C_p ($\mathrm{JK^{-1}\,mol^{-1}}$)	T (K)	C_p ($\mathrm{JK^{-1}\,mol^{-1}}$)	T (K)	C_p ($\mathrm{JK^{-1}\,mol^{-1}}$)
80.174	16.620	149.582	40.302	202.312	52.376	281.419	68.544
83.653	17.724	151.642	40.861	205.911	53.122	285.190	69.520
86.976	19.260	153.779	41.103	209.503	53.917	289.482	70.241
90.174	20.782	155.850	41.616	213.034	55.069	294.290	71.254
93.302	21.761	157.911	42.417	216.571	55.770	299.103	71.940
96.258	22.840	160.858	42.691	220.053	56.381	303.789	72.927
100.011	24.149	163.947	43.360	223.472	57.343	308.540	73.773
103.263	25.631	165.946	43.872	226.832	58.094	313.264	75.490
106.580	26.568	167.935	44.674	230.191	59.138	317.819	76.288
109.822	28.062	169.941	45.044	233.960	59.474	322.401	77.243
114.171	29.504	172.230	45.580	238.071	60.351	326.924	78.389
117.710	30.578	173.659	46.352	242.132	61.062	331.436	79.463
120.303	31.592	176.233	46.931	246.214	61.830	335.903	80.431
122.732	32.260	179.650	47.504	250.241	62.573	340.422	81.744
125.024	32.873	182.769	48.047	254.242	63.013	344.769	82.921
127.385	33.812	185.328	48.676	258.241	64.055	349.180	83.657
131.511	34.982	187.941	49.182	262.117	64.822	353.521	84.643
136.972	36.546	190.495	50.064	266.061	65.435	357.878	85.579
142.424	38.444	193.024	50.389	269.950	66.541	362.154	86.322
145.304	39.088	195.587	50.491	273.774	66.978	366.438	87.259
147.440	39.533	198.657	51.603	277.661	67.689	370.642	88.535

TABLE 4
The Measured Heat Capacity Values of 14-nm Rutile TiO_2 Ultrafine Powder, C_p ($JK^{-1}mol^{-1}$) ($M = 79.8988$)

T (K)	C_p ($JK^{-1}mol^{-1}$)	T (K)	C_p ($JK^{-1}mol^{-1}$)	T (K)	C_p ($JK^{-1}mol^{-1}$)	T (K)	C_p ($JK^{-1}mol^{-1}$)
79.009	13.652	133.213	33.578	201.730	52.056	288.250	71.670
81.640	14.688	136.180	34.461	205.864	53.113	292.603	72.813
84.127	15.644	139.089	35.430	209.991	54.271	297.027	73.512
86.554	16.355	141.204	36.155	214.047	55.228	301.314	74.675
88.951	17.263	144.927	37.072	218.104	56.101	305.576	75.682
91.233	18.388	147.661	37.744	222.008	57.034	309.862	76.578
93.452	19.474	150.543	38.351	225.603	58.122	314.071	77.782
95.658	20.311	153.272	39.367	229.826	58.857	318.340	78.469
97.801	20.889	155.604	40.151	233.742	60.144	322.478	79.752
100.014	21.701	158.726	41.167	237.501	60.784	326.530	80.537
102.083	22.577	161.380	41.873	241.329	61.563	330.661	81.354
104.066	23.742	164.259	42.392	245.080	62.290	334.724	82.512
106.352	24.447	167.433	43.155	248.812	63.059	338.703	83.606
108.914	25.430	170.531	44.190	252.547	63.952	342.759	84.524
111.470	26.293	173.554	44.950	256.313	64.667	346.674	85.619
113.966	27.021	176.576	45.704	259.934	65.281	350.650	86.672
116.329	28.228	179.532	46.812	263.608	66.155	354.662	87.871
118.809	28.794	182.480	47.455	267.230	66.588	358.621	88.837
121.230	29.631	185.503	48.323	270.921	67.403	363.863	90.015
124.004	30.537	189.039	49.127	274.903	68.332	367.906	91.122
127.118	31.563	193.391	50.289	279.402	69.644		
130.161	32.411	197.604	51.282	283.828	70.659		

For 75-nm ultrafine powder in the rutile phase,

$$C_p = 45.949 + 22.229X - 8.5445X^2 + 4.9229X^3 + 1.8171X^4 \quad (J\,K^{-1}\,mol^{-1}), \qquad [3]$$

where $X = (T - 223.89)/144.91$.

For the bulk crystal TiO_2 in the anatase phase,

$$C_p = 37.338 + 24.579X - 8.9290X^2 + 0.34322X^3 + 2.0624X^4 \quad (J\,K^{-1}\,mol^{-1}), \qquad [4]$$

where $X = (T - 175.33)/122.83$.

For the bulk crystal TiO_2 in the rutile phase,

$$C_p = 37.306 + 26.016X - 9.4791X^2 - 1.6680X^3 + 2.9885X^4 \quad (J\,K^{-1}\,mol^{-1}), \qquad [5]$$

where $X = (T - 175.33)/122.83$.

Equations [1], [2], and [3] are valid in the temperature range from 78 to 370 K, and Eqs. [4] and [5] from 52.5 to 298.15 K. The correlation coefficients of the above fitting equations are $R^2 > 0.9998$.

3.5. Discussion of the Energy of Different TiO_2 Samples

It can be seen from Fig. 2 that smooth and continuously rising curves are obtained in the plots of heat capacity vs temperature for nanocrystalline TiO_2 ultrafine powder and that no phase transition or thermal anomaly appears. The C_p–T curves of different samples lie at different positions at the same temperature. This implies that the energy states of the samples are different at the same temperature.

There are three reasons that the energy states of 14-, 15-nm crystalline TiO_2 are the highest. First, their radii are the smallest. Based on the theory of surface energy, the smaller the particle radius is, the bigger the specific surface is, and the higher the free energy of the specific surface is, the higher the energy is. Therefore the bulk crystalline is in the most stable state and its energy is the lowest. Second, they have the biggest distortion. As shown in Section 3.3, the smaller the grain radius is, the bigger the distortion is. And generally, the bigger the distortion is, and the higher internal stress is, the higher the energy is. Third, it is known that the lattice energy of anatase TiO_2 is lower than that of the rutile TiO_2 at the same temperature in general. The lower the lattice energy is, the higher the energy is.

It can also been seen from Fig. 2 that the heat capacity of 75-nm nanocrystal TiO_2 in the rutile phase is quite close to that of bulk crystal. This shows that their energy is nearly the same.

The heat capacity curve of 14-nm TiO_2 ultrafine powder in mixed rutile and anatase phase is intercrossed with that of

TABLE 5
The Measured Heat Capacity Values of 75-nm Rutile TiO_2 Ultrafine Powder, C_p ($JK^{-1}\,mol^{-1}$) ($M = 79.8988$)

T (K)	C_p ($JK^{-1}\,mol^{-1}$)	T (K)	C_p ($JK^{-1}\,mol^{-1}$)	T (K)	C_p ($JK^{-1}\,mol^{-1}$)	T (K)	C_p ($JK^{-1}\,mol^{-1}$)
78.976	11.943	141.723	29.844	209.115	43.815	284.859	54.140
81.717	12.859	144.712	30.603	212.644	44.551	288.691	54.291
84.302	13.810	147.658	31.162	216.108	44.913	292.462	54.764
86.809	14.677	150.566	32.048	219.581	45.380	296.734	55.573
89.683	15.301	153.438	32.633	222.974	45.924	301.527	56.369
92.822	16.438	156.276	33.248	226.360	46.440	306.324	56.895
95.845	17.522	159.082	33.794	229.757	47.095	311.035	57.482
98.788	18.113	161.858	34.548	233.082	47.542	315.691	58.302
101.644	18.943	164.602	34.744	236.403	47.948	320.340	59.131
104.961	20.121	167.968	35.591	240.709	48.295	324.983	59.520
108.714	21.309	171.938	36.860	245.408	49.030	329.560	60.168
112.361	22.439	175.850	37.491	249.478	49.636	334.126	60.772
115.902	23.386	179.712	38.226	253.514	50.191	338.632	61.291
119.360	24.392	183.527	38.880	257.491	50.894	343.061	62.092
122.740	25.142	187.295	39.617	261.479	51.232	347.780	62.846
126.048	25.918	191.021	40.618	265.461	51.618	351.978	63.681
129.292	26.666	194.709	41.183	269.372	51.926	356.332	64.345
132.478	27.488	198.361	41.728	273.280	52.391	360.679	64.901
135.609	28.206	201.983	42.039	277.191	53.220	364.821	65.372
138.689	28.847	205.569	43.172	281.023	53.723	368.803	66.119

15-nm TiO_2 ultrafine powder in anatase phase, and their curves are normal in lower temperature but abnormal in higher temperature. It is likely that these phenomena have close connection with the grain surface curvature and the internal stress applied to the lattice distortion. These problems are currently being studied.

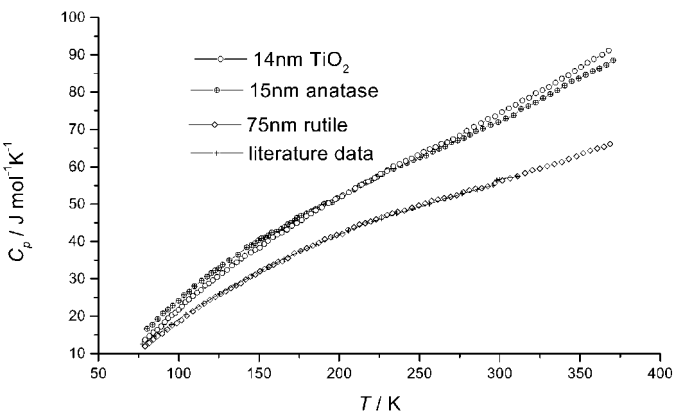

FIG. 2. The heat capacity–temperature curve of TiO_2 with various crystal grain sizes.

ACKNOWLEDGMENT

This work was financially supported by the National Nature Science Foundation of China under NSFC grant no. 29773048.

REFERENCES

1. L. D. Birkefeld, A. M. Azad, and S. A. Akbar, *J. Am. Ceram. Soc.* **75,** 2964 (1992).
2. Q. F. Zhou, S. H. Wu, Q. Q. Zhang, J. X. Zhang, J. Chen, and W. H. Zhang, *Chin. Phys. Lett.* **14,** 306 (1997).
3. M. Egon and M. Louis, *J. Colloid Interface Sci.* **6,** 302 (1997).
4. S. Doeuff, M. Henry, C. Sanchez, and J. Livage, *J. Non-Cryst. Solids* **89,** 206 (1987).
5. E. Haro-Poniatoski, R. Rodriguez-Talavera, M. de la Cruz Heredia, O. Cano-Corona, and R. Arroyo-Murillo, *J. Mater. Res.* **9,** 2102 (1994).
6. Z. C. Tan, G. Y. Sun, Y. Sun, A. X. Yin, W. B. Wang, J. C. Ye, and L. X. Zhou, *J. Thermal Anal.* **45,** 59 (1995).
7. X. M. Wu, Z. C. Tan, Y. J. Song, S. H. Meng, and S. S. Qu, *Thermochim. Acta* **346,** 57 (2000).
8. W. H. Zachariasen, "Theory of X-Ray Diffraction in Crystals." Wiley, New York, 1945.
9. L. S. Birks and H. Friedman, *J. Appl. Phys.* **17,** 687 (1946).
10. F. H. Chung, *J. Appl. Crystallogr.* **7,** 519 (1974).
11. C. H. Shomate, *J. Am. Chem. Soc.* **69,** 218 (1947).
12. Z. C. Tan, L. X. Zhou, D. X. Chen, A. X. Yin, Y. Sun, J. C. Ye, and X. K. Wang, *Sci. Sin. Ser. B* **26,** 1014 (1983).